

Single-exposure super-resolved interferometric microscopy by red–green–blue multiplexing

Alejandro Calabuig,¹ Vicente Micó,^{1,*} Javier Garcia,¹ Zeev Zalevsky,² and Carlos Ferreira¹

¹Departamento de Óptica, University Valencia, C/ Dr. Moliner, 50, 46100 Burjassot, Spain

²School of Engineering, Bar-Ilan University, 52900 Ramat-Gan, Israel

*Corresponding author: vicente.mico@uv.es

Received November 12, 2010; revised January 5, 2011; accepted February 16, 2011;
posted February 18, 2011 (Doc. ID 138137); published March 9, 2011

We present single-exposure super-resolved interferometric microscopy (SESRIM) as a novel approach capable of providing one-dimensional (1-D) super-resolution (SR) imaging in holographic microscopy using a single illumination shot. The single-exposure SR working principle is achieved by combining angular and wavelength multiplexing incoming from a set of tilted beams with different wavelengths where each wavelength is tuned with the red–green–blue (RGB) channels of a color CCD. Thus, the information included in each color channel is retrieved by holographic recording using a single-color CCD capture and by analyzing the RGB channels. Finally, 1-D SR imaging is obtained after the digital postprocessing stage yielding the generation of a synthetic aperture. Experimental results are reported validating the proposed SESRIM approach while an extension of the proposed approach to the two-dimensional case is considered. © 2011 Optical Society of America

OCIS codes: 100.2000, 100.6640, 170.1650, 180.3170.

Optical super-resolution (SR) relates to the capability to overcome the resolution limit of imaging systems imposed by the wave nature of light [1]. Such a limitation was first established by Abbe who, aside of explaining the role of NA and illumination wavelength (λ) concerning resolving power in microscopy, also pointed out that the resolution of an imaging system can be increased by tilting the illumination with respect to the optical axis [2]. Nearly one century later, Abbe's concept regarding resolution improvement was applied to holography by Ueda and Sato [3]. They reported on the recording of a multiexposed hologram comprising coherent addition of several bandpass images obtained sequentially under different oblique illuminations.

Since then, tilted beam illumination (or angular multiplexing) in combination with interferometric recording has been widely applied in digital holography [4–9] and digital holographic microscopy (DHM) [10–18] as a way to achieve SR imaging. But most of those approaches implement in time sequence the tilted beam illumination procedure [3–5,7,8,10,12–17]. This time multiplexing principle prevents the study of samples with fast events and dynamics since the sample should be static at least during the duration of the illumination stage (typically from some tenths of a second to a few seconds depending on system complexity and involved hardware). Nevertheless, other approaches exhibit or are theoretically valid for providing SR imaging in a single shot of the illumination source since they involve not time but rather coherence [6,11,13] or polarization [9,18] multiplexing. The single-exposure SR underlying principle enables the study of real-time events and becomes a highly attractive and applicable field of research.

In this Letter, we report on a novel strategy for providing single-exposure SR imaging in DHM where the payment for resolution improvement is done in the color domain. The approach, named single-exposure super-resolved interferometric microscopy (SESRIM), combines, for the first time to our knowledge, angular with wavelength multiplexing that are respectively responsible for the parallel transmission of different object spec-

tral bands through the limited system aperture and for the recovery of each transmitted band in a single recording of a color CCD when analyzing separately each one of its three red–green–blue (RGB) channels. Color object information is sacrificed to achieve an SR effect derived from a single CCD recording, recording three frequency bands in a single exposure.

The experimental setup is depicted in Fig. 1. Three beams simultaneously illuminate the sample with varied oblique coplanar directions: the red (R) beam illuminates in on-axis mode, while the blue (B) and green (G) beams reach the sample obliquely at angles of θ_B and θ_G , respectively. Because of this angular- and wavelength-multiplexed illumination stage, three elementary color-coded bandpass images, containing different spatial frequency content of the input sample, are simultaneously directed towards the digital recording device. At the output plane, a color CCD records three off-axis holograms incoming from the addition of the three elementary color-coded bandpass images plus the three off-axis reference beams (where each one is coherent with its corresponding bandpass image, and the incidence angle is set to avoid aliasing at the CCD peripheral area). Thus, information in a single color CCD capture concerning each transmitted color-coded bandpass image is retrieved by looking independently at the three RGB CCD channels. The image processing operations

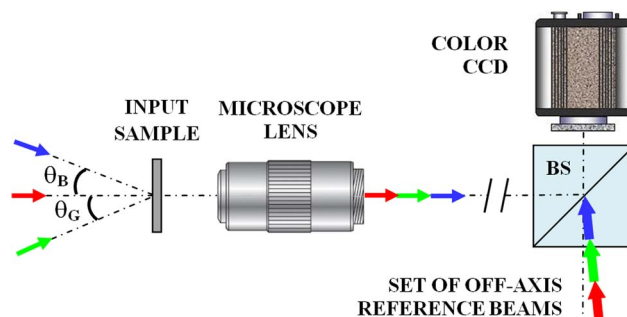


Fig. 1. (Color online) Experimental setup for SESRIM validation where BS is a beam splitter cube.

include Fourier transformation (FT) over each color-coded off-axis hologram, filtering one of the diffraction hologram orders, and inverse FT applied in order to come back again to the spatial domain. Once the three bandpass images are retrieved, or equivalently, the three shifted elementary apertures due to the tilted illumination, a synthetic aperture (SA) is generated, and a final one-dimensional (1-D) SR image is obtained by FT of the information contained in the SA.

Figure 2 schematizes the whole process involving SESRIM where the images are experimental results obtained when using a T-90 resolution test from Applied Image Inc. The images correspond with Group 3 of the test having eight elements consisting in 15 vertical bars per element and with spatial frequencies ranging from 100 to 500 line pairs/mm. First, the color-multiplexed recorded hologram is separated into its RGB channels. Because of chromatic aberration in the microscope lens, only one of the bandpass images will be focused at the CCD plane. In our case, we have focused the central bandpass image (on-axis illumination), and thus the off-axis bandpass images must be digitally refocused to guarantee good quality final SR imaging. For this reason, the following processing is performed on the G (left

column in Fig. 2) and B (right column in Fig. 2) channels: FT of the recorded channel hologram, filtering and centering the elementary aperture incoming from the first hologram diffraction order, digital propagation of the information contained in the recovered pupil to focus the bandpass image, and final inverse FT to retrieve the elementary aperture. The convolution approach applied to the diffraction Rayleigh–Sommerfeld integral has been used as digital propagation method [19]. Once the G and B elementary apertures are recovered, both are combined with the retrieved R channel aperture in order to assemble an SA incoming from the coherent addition of the individual pupils. The optimization process when adding the three elementary apertures is guided by a correlation operation, with the overlapping areas between elementary apertures presented in a similar way to [17]. Thus, the spatial frequency shifts at the Fourier domain, and the global phase differences and the amplitude ratios between elementary apertures are determined with pixel accuracy. Finally, SR imaging (lower right corner in Fig. 2) is obtained by FT of the generated SA in comparison with the conventional image obtained when only on-axis illumination is used (lower left corner in Fig. 2). As we can see, the resolution limit is improved from Element 4 (marked with white arrows, 200 line pairs/mm or $5\ \mu\text{m}$ pitch) to Element 8 (500 line pairs/mm or $2\ \mu\text{m}$ pitch), defining a resolution gain factor of 2.5.

Three lasers provide RGB coding for the experiments: an He–Ne laser source (632.8 nm laser wavelength, 35 mW optical power), a green-diode-pumped laser module (532 nm laser wavelength, 50 mW optical power), and a violet laser diode module (405 nm laser wavelength, 50 mW optical power). A long-working-distance infinity-corrected microscope lens (Mitutoyo M Plan Apo 0.14NA 5 \times) and a color CCD camera (AVT 1394 Stingray F-145C, 1388 \times 1038 pixels, 6.45 \times 6.45 μm pixel pitch) are used as imaging lens and recording device, respectively.

The illumination angles for the G and B tilted beams are $\theta_G = 13.5^\circ$ and $\theta_B = 12^\circ$, respectively. Note that both values are slightly below the angle defined by twice the NA angle of the microscope lens (8.05°). This fact guarantees a given spectral area overlapping between recovered elementary apertures when generating the SA. Moreover, since diffraction is wavelength dependent [2], the information contained in the G and B apertures is higher than for the R case. Thus, the size of the

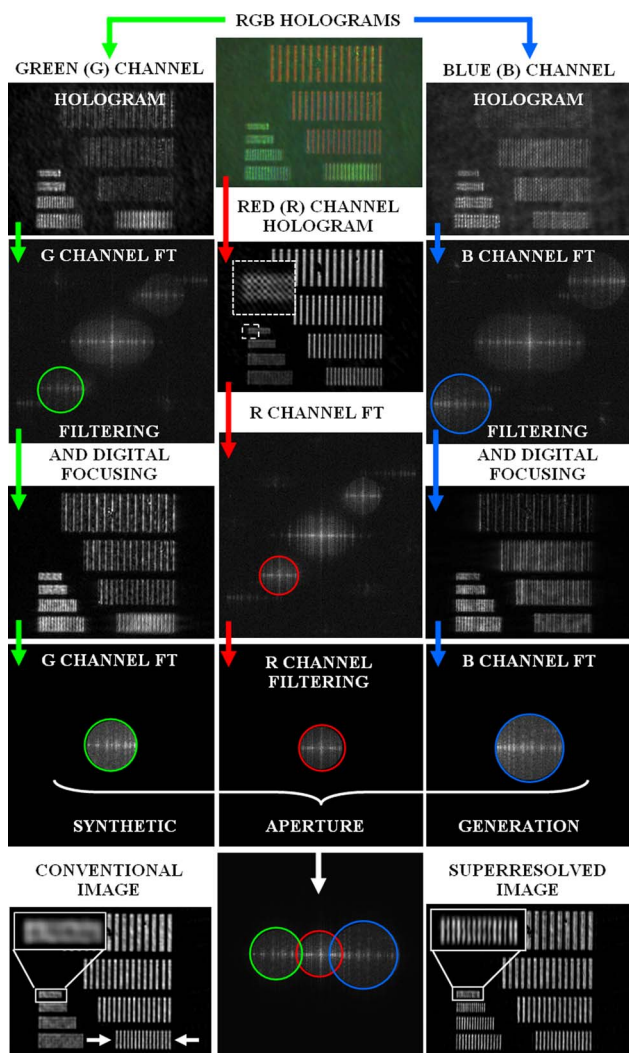


Fig. 2. (Color online) Schematic chart of the SESRIM approach.

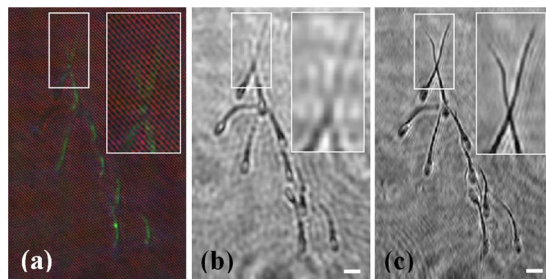


Fig. 3. (Color online) Experimental results using a swine sperm biosample: (a) the RGB holograms, (b) the conventional image, (c) the SR image. Scale bars in cases (b) and (c) are $10\ \mu\text{m}$.

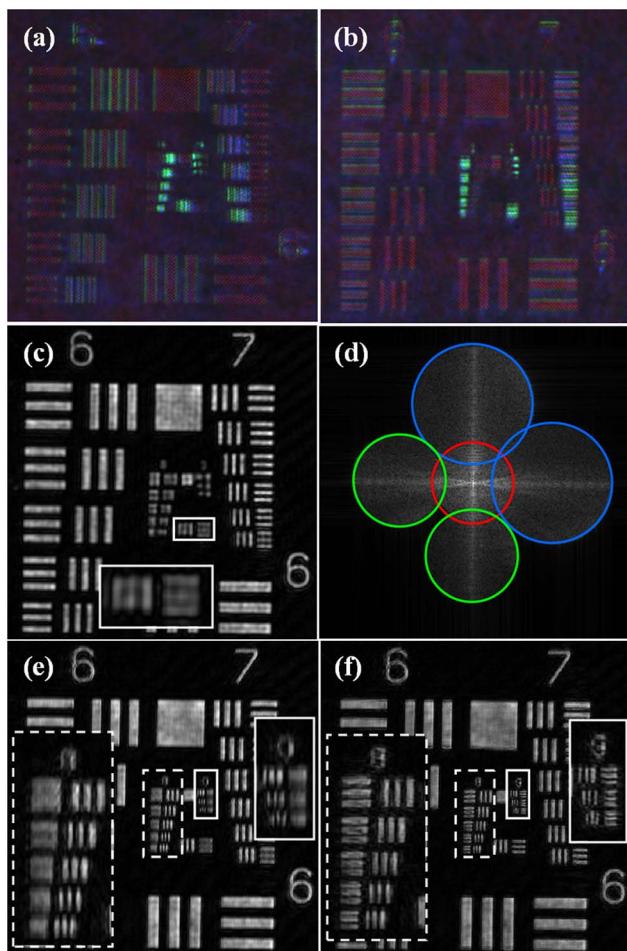


Fig. 4. (Color online) Two-dimensional extension of the proposed method by using time multiplexing: (a), (b) the horizontal and vertical RGB holograms, respectively, (c) the conventional low-resolution image, (d) the generated SA, and (e), (f) the super-resolved images in 1-D and 2-D, respectively. The insets show magnified regions of the images to clearly visualize the SR effect.

elementary pupil increases as the wavelength decreases, providing an improvement in the overlapping spectral area. Overlapping between recovered pupils is needed for optimizing the SA generation according to the procedure here adopted [17]. However, correct reallocation of each aperture can also be guided visually without spectral overlapping [11,15] allowing maximum SA coverage.

The SESRIM approach has also been tested considering a biological sample comprising unstained swine sperm cells that are fixed by drying up the sample. The cells have an ellipsoidal head of $6 \times 9 \mu\text{m}$ and a tail's width of around $2 \mu\text{m}$ on the head side and below $1 \mu\text{m}$ on its end. Figure 3 depicts the experimental results where SESRIM allows imaging of the sperm tail that is not resolvable using a conventional imaging mode. The full complex amplitude is recovered, allowing further refocusing.

We have extended the proposed approach to the two-dimensional (2-D) case by rotating the object and using time multiplexing. Figure 4 depicts the results when considering a negative high-resolution United States Air Force test target: (a) and (b) show the horizontal and vertical RGB holograms, (c) presents the conventional im-

age when only R illumination channel is considered, (d) depicts the 2-D SA generated from the two 1-D SAs provided by SESRIM when considering a 90° rotation of the test between the recordings, (e) shows the 1-D SR image provided by SESRIM only in the horizontal direction, and (f) shows the 2-D SR image when the two 1-D SR orthogonal images are combined. Note that the resolution limit is again improved by a factor of 2.5 in both orthogonal directions since the last resolved element passes from Group 8–Element 1 (256 line pairs/mm or $3.9 \mu\text{m}$ pitch) to Group 9–Element 3 (645 line pairs/mm or $1.55 \mu\text{m}$ pitch). The 2-D Fourier domain coverage can be made with two exposures instead of the five that would be required without multiplexing. For a real valued sample (with symmetric spectrum that requires recording only half of the Fourier domain), one shot would still be possible.

In summary, we have reported on SESRIM as a new approach to allow 1-D SR instantaneous effect in coherent microscopic imaging based on wavelength multiplexing by an RGB illumination–detection scheme. Experiments have been performed for both synthetic and biological samples, and 2-D case by time multiplexing has been validated.

This work has been supported by the Spanish Ministerio de Educación y Ciencia under the project FIS2010-16646. We thank Professor Carles Soler and Paco Blasco from Proiser Research and Development S.L. for the swine sperm sample.

References

1. Z. Zalevsky and D. Mendlovic, *Optical Super Resolution* (Springer, 2002).
2. E. Abbe, *Archiv. Mikr. Anat.* **9**, 413 (1873).
3. M. Ueda and T. Sato, *J. Opt. Soc. Am.* **61**, 418 (1971).
4. T. Sato, M. Ueda, and G. Yamagishi, *Appl. Opt.* **13**, 406 (1974).
5. S. A. Alexandrov, T. R. Hillman, T. Gutzler, and D. D. Sampson, *Phys. Rev. Lett.* **97**, 168102 (2006).
6. C. Yuan, H. Zhai, and H. Liu, *Opt. Lett.* **33**, 2356 (2008).
7. V. Mico and Z. Zalevsky, *J. Biomed. Opt.* **15**, 046027 (2010).
8. L. Granero, V. Micó, Z. Zalevsky, and J. García, *Appl. Opt.* **49**, 845 (2010).
9. J. Zhao, X. Yan, W. Sun, and J. Di, *Opt. Lett.* **35**, 3519 (2010).
10. C. J. Schwarz, Y. Kuznetsova, and S. R. J. Brueck, *Opt. Lett.* **28**, 1424 (2003).
11. V. Mico, Z. Zalevsky, P. García-Martínez, and J. García, *Opt. Express* **12**, 2589 (2004).
12. V. Mico, Z. Zalevsky, and J. García, *Opt. Express* **14**, 5168 (2006).
13. V. Mico, Z. Zalevsky, P. García-Martínez, and J. García, *J. Opt. Soc. Am. A* **23**, 3162 (2006).
14. Y. Kuznetsova, A. Neumann, and S. R. J. Brueck, *Opt. Express* **15**, 6651 (2007).
15. V. Mico, Z. Zalevsky, C. Ferreira, and J. García, *Opt. Express* **16**, 19260 (2008).
16. V. Mico, Z. Zalevsky, and J. García, *Opt. Commun.* **281**, 4273 (2008).
17. J. Bühl, H. Babovsky, A. Kiessling, and R. Kowarschik, *Opt. Commun.* **283**, 3631 (2010).
18. C. Yuan, G. Situ, G. Pedrini, J. Ma, and W. Osten, *Appl. Opt.* **50**, B6 (2011).
19. T. Kreis, *Handbook of Holographic Interferometry: Optical and Digital Methods* (Wiley-VCH, 2005).